Stem Cell Research (2011) 6, 226–237

available at www.sciencedirect.com

ScienceDirect

www.elsevier.com/locate/scr

REGULAR ARTICLE

In vitro culture and characterization of putative porcine embryonic germ cells derived from domestic breeds and Yucatan mini pig embryos at Days 20–24 of gestation

Stoyan G. Petkov[a,*], Hendrik Marks[b,1], Tino Klein[c,1], Rodrigo S. Garcia[c], Yu Gao[a], Henk Stunnenberg[b], Poul Hyttel[a]

[a] *Department of Basic Animal and Veterinary Sciences, University of Copenhagen, Denmark*
[b] *Department of Molecular Biology, Nijmegen Centre for Molecular Life Sciences (NCMLS), Radboud University, The Netherlands*
[c] *Novo Nordisk A/S, Denmark*

Received 7 December 2010; received in revised form 18 January 2011; accepted 18 January 2011
Available online 31 January 2011

Abstract Embryonic germ cells (EGC) are cultured pluripotent cells derived from primordial germ cells (PGC). This study explored the possibility of establishing porcine EGC from domestic breeds and Yucatan mini pigs using embryos at Days 17–24 of gestation. In vitro culture of PGC from both pooled and individual embryos resulted in the successful derivation of putative EGC lines from Days 20 to 24 with high efficiency. RT-PCR showed that gene expression among all 31 obtained cell lines was very similar, and only minor changes were detected during in vitro passaging of the cells. Genome-wide RNA-Seq expression profiling showed no expression of the core pluripotency markers *OCT4*, *SOX2*, and *NANOG*, although most other pluripotency genes were expressed at levels comparable to those of mouse embryonic stem cells (ESC). Moreover, germ-specific genes such as *BLIMP1* retained their expression. Functional annotation clustering of the gene expression pattern of the putative EGC suggests partial differentiation toward endo/mesodermal lineages. The putative EGC were able to form embryoid bodies in suspension culture and to differentiate into epithelial-like, mesenchymal-like, and neuronal-like cells. However, their injection into immunodeficient mice did not result in teratoma formation. Our results suggest that the PGC-derived cells described in this study are EGC-like, but seem to be multipotent rather than pluripotent cells. Nevertheless, the thorough characterization of these cells in this study, and especially the identification of various genes and pathways involved in pluripotency by RNA-Seq, will serve as a rich resource for further derivation of porcine EGC.

* Corresponding author at: Institute for Farm Animal Genetics, Mariensee, Friedrich-Loeffler-Institute (FLI), Höltystrasse 10, 31535 Neustadt, Germany. Fax: +49 05034 871 143.
E-mail address: petkov@tzv.fal.de (S.G. Petkov).
[1] These authors contributed to an equal extent to this work.

1873-5061/$ – see front matter
doi:10.1016/j.scr.2011.01.003

Introduction

Establishment of embryonic stem cells (ESC) in the farm animal species would benefit animal health and provide relevant models for developing regenerative therapies in humans. However, despite over two decades of ongoing research, no stable long-term ESC lines with preserved pluripotent characteristics have been reported in the pig (for reviews, see Brevini et al., 2008; Hall, 2008; Keefer et al., 2007; Vaskova et al., 2007). Embryonic germ cells (EGC), which are cultured pluripotent stem cells derived from primordial germ cells (PGC), have been established in the mouse (Matsui et al., 1992; Resnick et al., 1992) and shown to possess morphological and pluripotent characteristics similar to mouse ESC, including ability to reenter the germ line (Labosky et al., 1994; Stewart et al., 1994). In addition, EGC derivation has been reported in other species, including pig (Müller et al., 1999; Piedrahita et al., 1998; Shim et al., 1997; Tsung et al., 2003; Petkov and Anderson, 2008). Hence, porcine EGC could be considered as an alternative to ESC.

The conversion of PGC into pluripotent stem cells in culture is a poorly understood process. Mouse PGC are unipotent, i.e., not capable of differentiation into somatic cell types and contributing to chimeras, and acquire pluripotency only after a certain period in culture (Stewart et al., 1994; Durcova-Hills et al., 2006). For their survival and proliferation in vitro they require the presence of leukemia inhibitory factor (LIF), stem cell factor (SCF), and basic fibroblast growth factor (bFGF) in the culture medium (Matsui et al., 1992; Resnick et al., 1992). As a ligand of c-kit, SCF is essential for survival of mouse PGC in vivo and in vitro by inhibiting apoptosis (Pesce et al., 1993; Sette et al., 2004), while LIF is necessary for maintenance of pluripotency. It has been shown that bFGF plays an important role for in vitro reprogramming of mouse PGC (Durcova-Hills et al., 2006). Furthermore, B lymphocyte-induced maturation protein 1 (BLIMP1/PRDM1), a transcriptional repressor critical for the specification of the germ line (Hayashi et al., 2007; Ohinata et al., 2005; Saitou et al., 2005), downregulates the transcription of *c-myc* and Krüppel-like factor 4 (*Klf4*) in mouse PGC, in addition to preventing their differentiation into the somatic lineages. Downregulation of BLIMP1 by bFGF in culture allows the expression of *c-myc* and *Klf4* to be upregulated, which in turn leads to reprogramming of mouse PGC to attain pluripotency (Durcova-Hills et al., 2008). Both *c-myc* and *Klf4* are transcription factors that together with Octamer binding protein 4 (*Oct4*) and SRY-box 2 protein (*Sox2*) are capable of reprogramming somatic cells into induced pluripotent stem cells (iPSC) (Takashi and Yamanaka, 2006; Takashi et al., 2007; Okita et al., 2007).

Unlike in the mouse, freshly isolated porcine PGC are capable of contributing to somatic chimeras (Müller et al., 1999) and to survive and to proliferate in serum-supplemented and in serum-free culture without any growth factor supplementation (Shim et al., 1997; Petkov and Anderson, 2008). It is therefore unclear if the same mechanisms of reprogramming occur in porcine PGC when placed in culture. The EGC lines derived from these porcine cells have shown the ability to differentiate into cells from the three germ layers in vitro and also upon injection into blastocysts (Müller et al., 1999; Piedrahita et al., 1998; Shim et al., 1997). However, these EGC have been characterized for relatively few pluripotency markers and have not shown sufficient evidence for pluripotency such as germ-line chimera formation in vivo (likely due to the relatively low extent of chimeric contribution), or ability for indefinite self-renewal in vitro, two important criteria for pluripotent embryonic stem cells. Therefore, an improvement of the culture conditions for derivation and propagation of porcine EGC as well as more systematic application of all relevant methods for characterization of these cells is currently necessary.

The stage of embryonic development has been shown to be a decisive factor in the derivation of EGC in the mouse, where these cells have been derived from Day 8.5–13.5 embryos (Matsui et al., 1992; Resnick et al., 1992; Labosky et al., 1994; Durcova-Hills et al., 1999; Durcova-Hills et al., 2001; Durcova-Hills et al., 2004; Tada et al., 1998; Shim et al., 2008). To date, porcine EGC have been derived from embryos at Days 24–25 (Shim et al., 1997), 25–27 (Piedrahita et al., 1998), and 26–28 (Tsung et al., 2003). Derivation of EGC lines from later stage embryos may be limited due to the fact that soon after arrival to the genital ridge, male and female PGC undergo mitotic and meiotic arrest, respectively (Buehr, 1997). In contrast, the use of younger embryos for EGC culture might help to improve the efficiency of derivation as well as the quality of the established EGC lines, since PGC at earlier stages of development may have a higher proliferative potential than those in the genital ridge. At the same time, migrating PGC are less advanced in the process of gametogenesis and therefore closer to the pluripotent epiblast from which they descend.

In this study we explored the possibility of deriving porcine EGC from pooled and individual embryos at Days 17–24 of pregnancy from Danish Landrace × Yorkshire crosses and Yucatan mini pig. Successfully established putative EGC lines from embryos at Days 20–24 of gestation were characterized and tested for pluripotency using a variety of methods.

Results

Derivation and morphology of putative EGC colonies

The results from the derivation of lines from PGC at the different embryonic stages are summarized in Table 1. Putative EGC colonies formed in all primary cultures from embryos at Days 17–18 of pregnancy, but were lost during the three subsequent passages. All cultures from 20- to 24-day-old embryos formed numerous compact colonies, which proliferated actively and allowed multiple cell lines to be established from pooled as well as from individual embryos. The overall efficiency of putative EGC derivation from individual and pooled primary cultures was 74 and 100%, respectively. All nine cultures established from Yucatan mini pig PGC resulted in the derivation of putative EGC lines. All cell lines proliferated for over 10 passages without showing any signs of senescence. Three cell lines were maintained for over 30 passages, after which their proliferation slowed down and stopped by passage 35. The derived putative EGC colonies had a round/oval-shaped and flat but compact appearance. There was no difference in the colony morphology between cultures from Landrace × Yorkshire crosses (Figs. 1A and B) and Yucatan mini pig (Fig. 1C).

Transmission and scanning electron microscopy

At passage 4, the putative EGC colonies were of varying sizes. At least from scanning electron microscopy (SEM), larger colonies displayed a peripheral elevated zone (Fig. 1D). Each colony consisted of tightly clustered rounded cells adherent to each other by intermediate junctions and tight junctions (Figs. 1E and F). The cells displayed abundant rough endoplasmic reticulum and mitochondria, and in the

Table 1 Efficiency of putative EGC line derivation from different embryonic stages.

Breed	Embryo stage, days	Embryos, No.	Primary cultures, No.		Cell lines, No. (%)
Landrace × Yorkshire	17–18	31	Pooled	2	0 (0)
			Individual	14	0 (0)
Landrace × Yorkshire	20–21	47	Pooled	2	2 (100)
			Individual	15	8 (53)
Landace × Yorkshire	22–24	65	Pooled	3	3 (100)
			Individual	11	9 (81)
Yucatan mini pig	23–24	9	Individual	9	9 (100)

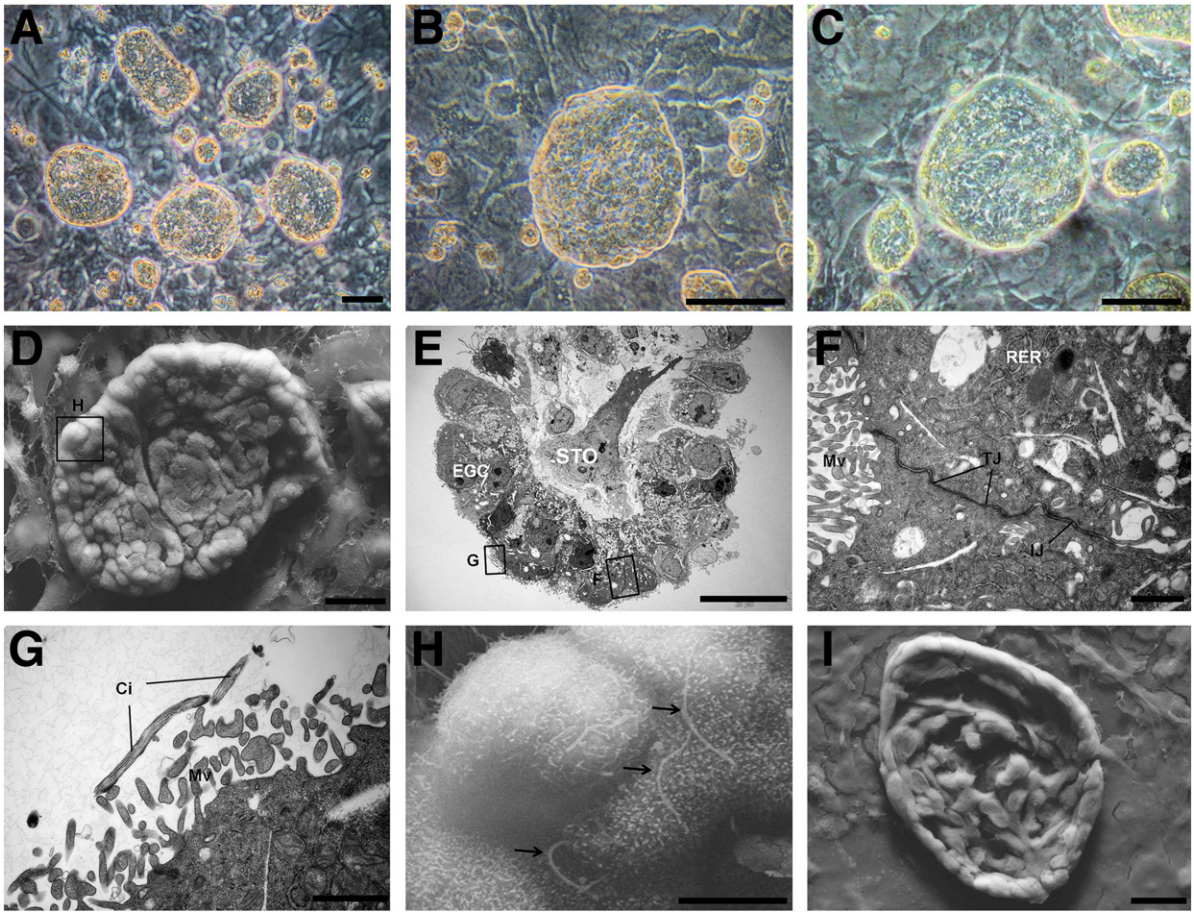

Figure 1 Morphologies of putative embryonic germ cells (EGC) derived from Landrace × Yorkshire and Yucatan mini pig embryos. (A and B) Morphology of putative EGC lines derived from Landrace × Yorkshire crosses (scale bars = 50 μm). (C) Putative EGC derived from Yucatan mini pig embryos (scale bar = 50 μm). (D) Scanning electron micrograph of passage 4 colony growing on feeder cells (STO). Note the thickened peripheral portion of the colony (scale bar = 20 μm). (E) Transmission electron micrograph of passage 4 colony growing on feeder cells (STO) (scale bar = 20 μm). (F) Boxed area from E. Adjacent EGC are connected by intermediate junctions (IJ) and tight junctions (TJ) and display rough endoplasmic reticulum (RER) (scale bar = 1 μm). (G) Boxed area from E. The embryonic germ cells are covered by microvilli (Mv) and present primary cilia (Ci) (scale bar = 1 μm). (H) Boxed area from D. Note the primary cilia (arrows) extending from each cell (scale bar = 5 μm). (I) Scanning electron micrograph of passage 8 putative EGC growing on feeder cells (STO). Note the more elongated shape of the EGC as compared with D (scale bar = 20 μm).

basolateral cell compartment, a massive population of vesicles containing more or less electron-dense material was observed (Figs. 1E and F). The surface of the putative EGC was covered with microvilli (Figs. 1F and G), and a primary cilium was observed to extend from a majority of the cells (Figs. 1G and H). Our SEM observations at later passages (P8 and 9) demonstrated that the cells, at least in some putative EGC colonies, had attained a slightly more elongated shape and had lost the primary cilia (Fig. 1I). In other colonies, the rounded cell shape was preserved and primary cilia were still present.

Gene expression of primary cultures and continuous cell lines

Analysis of gene expression in two primary cultures and 10 lines at P6-7 by RT PCR and RNA-Seq did not show any significant presence of transcripts for *POU5F1 (OCT4)*, *SOX2*, *NANOG*, and *ZFP42 (REX1)*. However, we detected transcripts for *C-MYC*, *KLF4*, *TERT*, *E-Cadherin*, *CDH1*, and *BLIMP1* (Fig. 2A). There was the presence of transcripts for *TDH* in the primary cultures, but not in any of the P6–7 samples. In addition, we detected strong bands for *LIFr*, *gp139*, and *STAT3* in most of the cell lines, in addition to weaker bands for *FGFr1* and *FGFr2* (Fig. 2B). The *C-KIT* receptor was detected only in primary culture colonies, but was almost undetected at later passages. The expression patterns of all analyzed genes were very similar in all of the characterized cell lines, suggesting that the methods for PGC isolation and culture allowed for consistent and reproducible results.

In the process of characterizing *NANOG* expression we found that all putative EGC lines expressed high levels of a transcript with high homology to *NANOG*, which we identify as putative pseudogene due to the presence of stop codons close to the transcription start (GenBank Accession Number AK231434; (Uenishi et al., 2004)). Due to high sequence similarity, this transcript was amplified together with *NANOG* by most of our primers. For that reason, we designed a reverse primer binding to a region of low sequence homology and were able to achieve *NANOG*-specific amplification. The transcript levels of *NANOG* were much lower compared with sequence AK231434 (data not shown).

RNA-Seq analysis

To further characterize the putative EGC, we performed genome-wide transcriptome profiling using RNA-Seq. For comparative purposes, we also performed RNA-Seq profiling on pig embyo

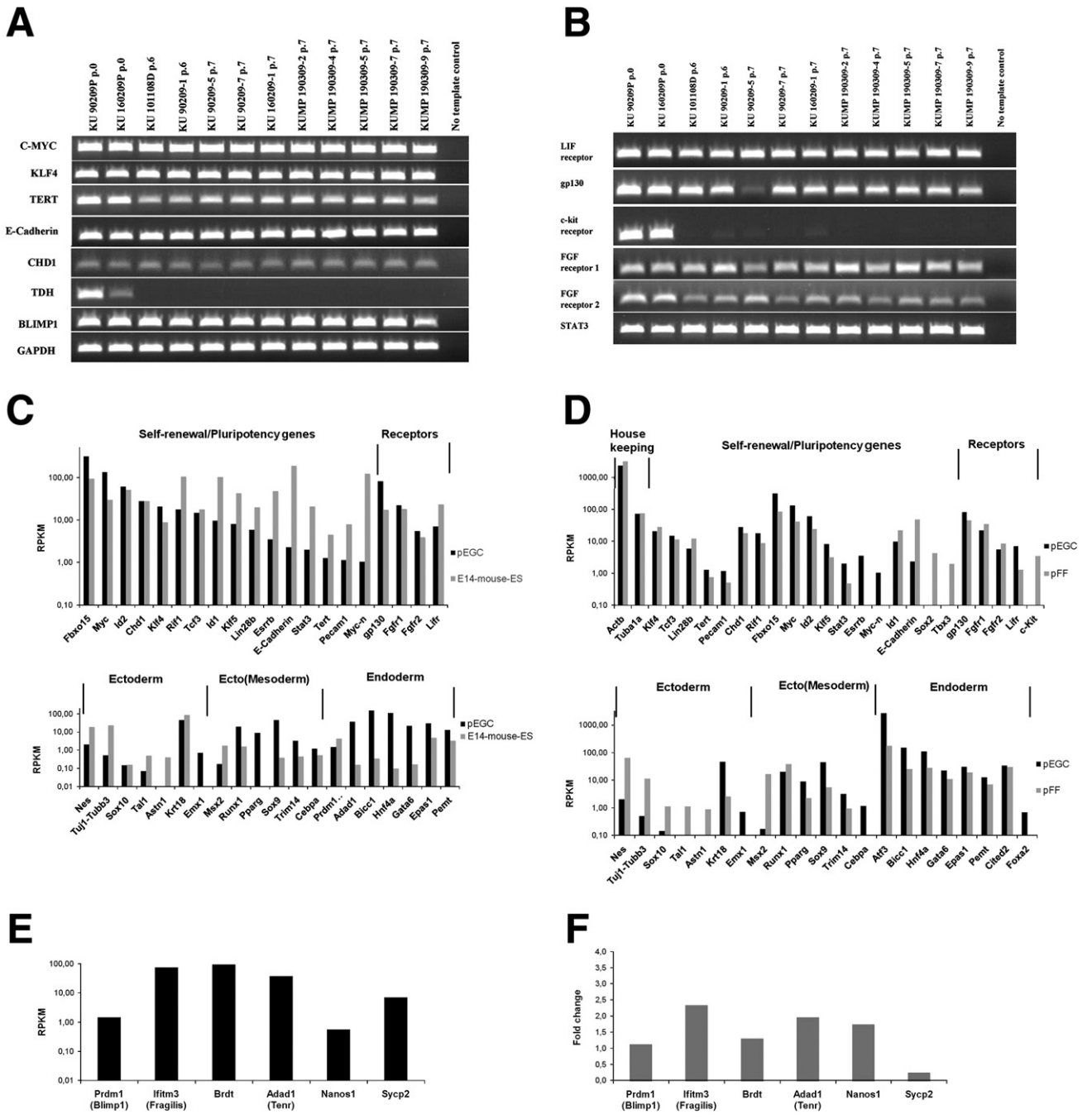

Figure 2 Analysis of gene expression in putative EGC by RT-PCR and RNA-Seq. (A) Expression of pluripotency and germ cell markers (RT-PCR). The first two columns are from primary cultures, columns 3–7 show results for five lines derived from Danish Landrace crosses, and columns 8–12 show the results for five lines derived from Yucatan mini pig. (B) Expression of receptors for leukemia inhibitory factor (LIF), fibroblasts growth factor (FGF), and stem cell factor (SCF) signaling (RT-PCR). (C) Expression of genes associated with pluripotency (upper panel) and differentiation (lower panel) in putative pig EGC and mouse ESC (RNA-Seq). (D) Expression of genes associated with pluripotency (upper panel) and differentiation (lower panel) in putative porcine EGC and pig fetal fibroblasts (pFF) (RNA-Seq). (E) Expression of germ-line-specific genes in putative pEGC (RNA-Seq). (F) Comparison of the germ-line-specific gene expression between putative EGC and pFF. The differences are shown as fold upregulation in putative EGC vs pFF. RPKM—Reads Per Kilobase of exon model per Million mapped reads.

fibroblasts (pFF). Figure S1 shows a snapshot of the data on two housekeeping genes as well as on two genes on chromosome 5, showing the anticipated signals specifically over the exons of genes. For further analysis, we summed the number of tags over coding bodies of the genes to obtain quantitative gene expression values (RPKM; see Materials and methods).

To gain an insight in the stemness of the putative EGC, we compared these to the well-characterized mouse E14 ESC and

compared a panel of genes which are known to be important for pluripotency and/or self-renewal (Mikkelsen et al., 2007). Surprisingly, the putative porcine EGC showed no expression of the pig orthologs for *Pou5f1*, *Nanog*, *Sox2*, and *Rex1*, the expression of which in human and mouse stem cells is considered the hallmark of pluripotency and self-renewal (Table S2A). However, we detected various other genes important for self-renewal and pluripotency in mouse, such as *KLF4, KLF5*, *ESSRB,* and *TERT* (Fig. 2C, upper panel), indicating that at least some pluripotency markers are conserved and showing the multipotent character of the putative EGC. Also the *LIFr* and *FGF1/2r* genes, which encode receptors of signaling pathways important for pluripotency in mouse and human, respectively, were highly expressed. Interestingly, orthologs of various ES cells markers that were shown to be important in mouse, such as *Klf2*, *Dppa2,* and *Id3*, seem to be absent in the pig (Table S2A). Finally, in addition to *BLIMP1*, we detected expression of the well-known germ-line-specific genes *IFITM3* (*FRAGILIS*), *BRDT*, *ADAD1* (*TENR*), *NANOS1*, and *SYCP2* (Fig. 2E). These genes also consistenly showed higher expression levels in putative EGC as compared to pFF (Fig. 2F).

To assess the differentiation of the putative EGC, we investigated the early lineage marker genes (Fig. 2C, lower panel). Mouse ESC are known to express some of these genes in undifferentiated state. Expression analysis showed that various early lineage markers which are expressed in mouse ESC were not expressed in putative EGC, such as the well -studied *Otx2*, *Neurog1*, *T* (*Brachyury*), and *Bmp2* (Table S2B). For the genes expressed in the putative EGC, we noted that mainly genes involved in endoderm and mesoderm development were expressed (also higher as compared with mouse ESC; Fig. 2C, lower panel), suggesting that the putative EGC may be partly differentiated into the endodermal/mesodermal lineage. Interestingly, various well-studied mouse lineage markers seem to lack orthologs in pigs (Table S2B).

Next, we compared the transcriptome of the putative EGC with pFF isolated from Day 23–24 porcine embryos (see Materials and methods; Fig. 2D; Fig. S4A). Most of the pluripotency markers showed similar expression in putative EGC and pFF (Fig. 2D, upper panel), although some showed lower expression in the pFF. Surprisingly, the pluripotency genes *SOX2* (Fig. S4A), *TBX3*, *E-Cadherin,* and *C-KIT* showed much higher expression in the pFF. The comparison for the lineage-specific genes (Fig. 2D, lower panel) also shows that genes from the ectoderm linage (e.g., *NES, SOX10*) are expressed higher in the pFF compared with the putative EGC, further suggesting ectodermal differentiation of the pFF (see Fig. S4B for four examples of lineage-specific genes). To compare the putative EGC and pFF on a genome-wide scale, we performed functional analysis (PANTHER) on all genes which are >2-fold differentially expressed between the putative EGC and the pFF (Table 2). The genes specific for putative EGC are mainly involved in metabolic processes, suggesting activity of additional metabolic pathways as compared with the pFF, while the genes specifically expressed in pFF show a strong, very significant enrichment of genes involved in developmental processes, and mainly for ectodermal and mesodermal development. This further confirms the ecto-/mesodermal signature of the pFF as suggested by Fig. 2D (lower panel). Expression of the individual genes present in both classes is shown in Fig. S2.

Alkaline phosphatase staining and immunocytochemistry

All putative EGC colonies possessed strong alkaline phosphatase activity (Fig. 3A). In line with our transcription data, we could not detect any above-background staining with antibodies against OCT4, SOX2, or NANOG. At the same time, all colonies stained positive for C-MYC (Fig. 3B). While none of the analyzed cultures reacted positively with SSEA-1 antibodies, most colonies had strong SSEA-4 staining on most of their surfaces (Fig. 3C). Only small parts of all colonies showed positive staining for TRA-1-60 (Fig. 3D) and TRA-1-81 (Fig. 3E) antigens. Lastly, the putative EGC colonies were positive for BLIMP1, although remarkably the localization of this protein did not appear to be restricted to nuclei (Fig. 3F).

In vitro differentiation

After 2 days in "hanging drop" culture, the putative EGC formed aggregates, and after 5 days most drops contained several simple EB that cavitated a few days later (Fig. 4A). Light microscopy of semithin sections showed an outer layer of large, endoderm-like epithelial cells surrounding an inner portion of mesenchymal-like cells embedded in abundant extracellular matrix (Fig. 4B). When allowed to attach on gelatin-treated surfaces, the putative EB proliferated extensively and formed outgrowths of mesenchymal-like (Fig. 4C), epithelial-like (Fig. 4D), and neuronal-like cells (Figs. 4E and F). Some of the differentiated cells reacted positively with antibodies against cytokeratin, Fox2A (Fig. 4G), vimentin (Fig. 4H), and beta III tubulin (Fig. 4I).

Teratoma testing

When immunodeficient mice were injected subcutaneously or intramuscularly with undifferentiated porcine putative EGC, tumor outgrowths could be discerned in both locations as early as Week 3.5 (intramuscular injection) and Week 5 (subcutaneous injection). Some tumors first developed after 10 weeks. In subcutaneously injected

Table 2 Functional analysis (PANTHER) on all genes >2-fold differential expressed between pEGCs and pFFs.

Genes specific for pEGC (>2 fold higher)				Genes specific for pFF (>2 fold higher)			
Functional term	Count	%	*P* value	Functional term	Count	%	*P* value
Other metabolism	185	4.4	3.70E-14	Developmental processes	333	21	1.00E-41
Lipid, fatty acid and other metabolism	236	5.6	2.90E-13	Cell communication	183	12	1.70E-23
Amino acid metabolism	83	2	4.80E-10	Ectoderm development	126	8.1	1.00E-21
Fatty acid metabolism	74	1.8	1.90E-09	Mesoderm development	109	7	4.10E-21
Electron transport	97	2.3	1.10E-08	Neurogenesis	112	7.2	9.90E-20
Intracellular signaling	229	5.4	1.40E-08	Skeletal development	39	2.5	6.70E-14
				Signal transduction	395	25	4.50E-10
				Ligand-mediated signaling	62	4	4.60E-09
				Cell adhesion	85	5.5	1.10E-08
				Cell adhesion-mediated signaling	61	3.9	3.30E-08
				Cell structure and motility	127	8.2	6.10E-08

Only terms with a *P* value of < 10E-7 are shown.

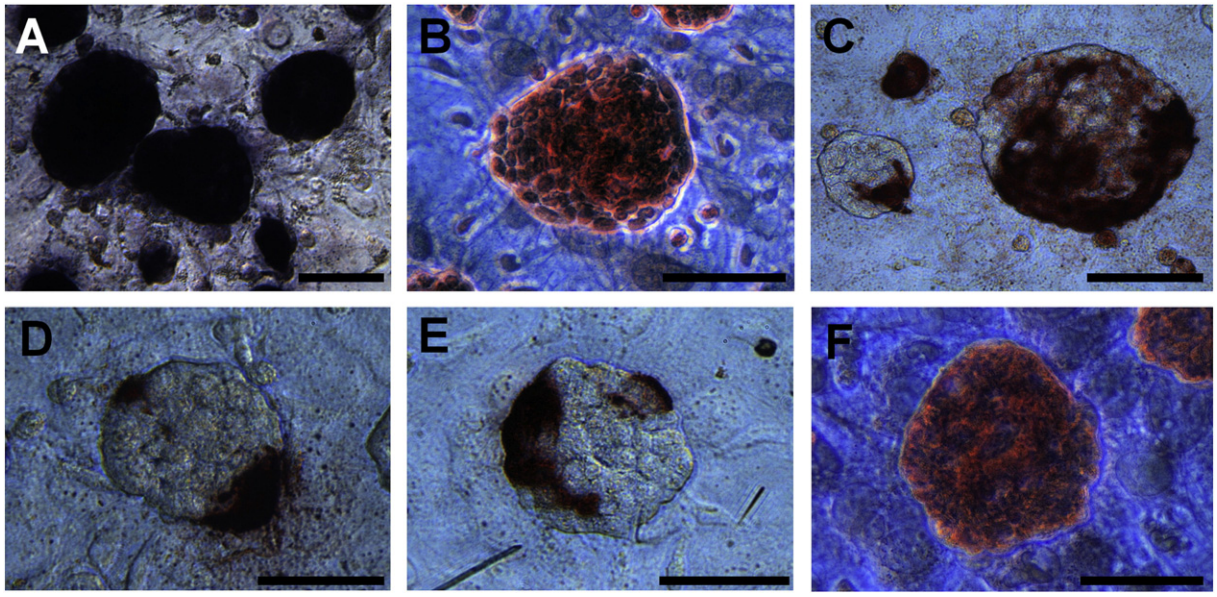

Figure 3 Alkaline phosphatase and immunocytochemical staining of putative porcine embryonic germ cells (EGC). (A) Alkaline phosphatase (dark blue). (B) C-MYC. (C) SSEA-4. (D) TRA1-60. (E) TRA-1-81. (F) BLIMP1 (all scale bars = 50 μm).

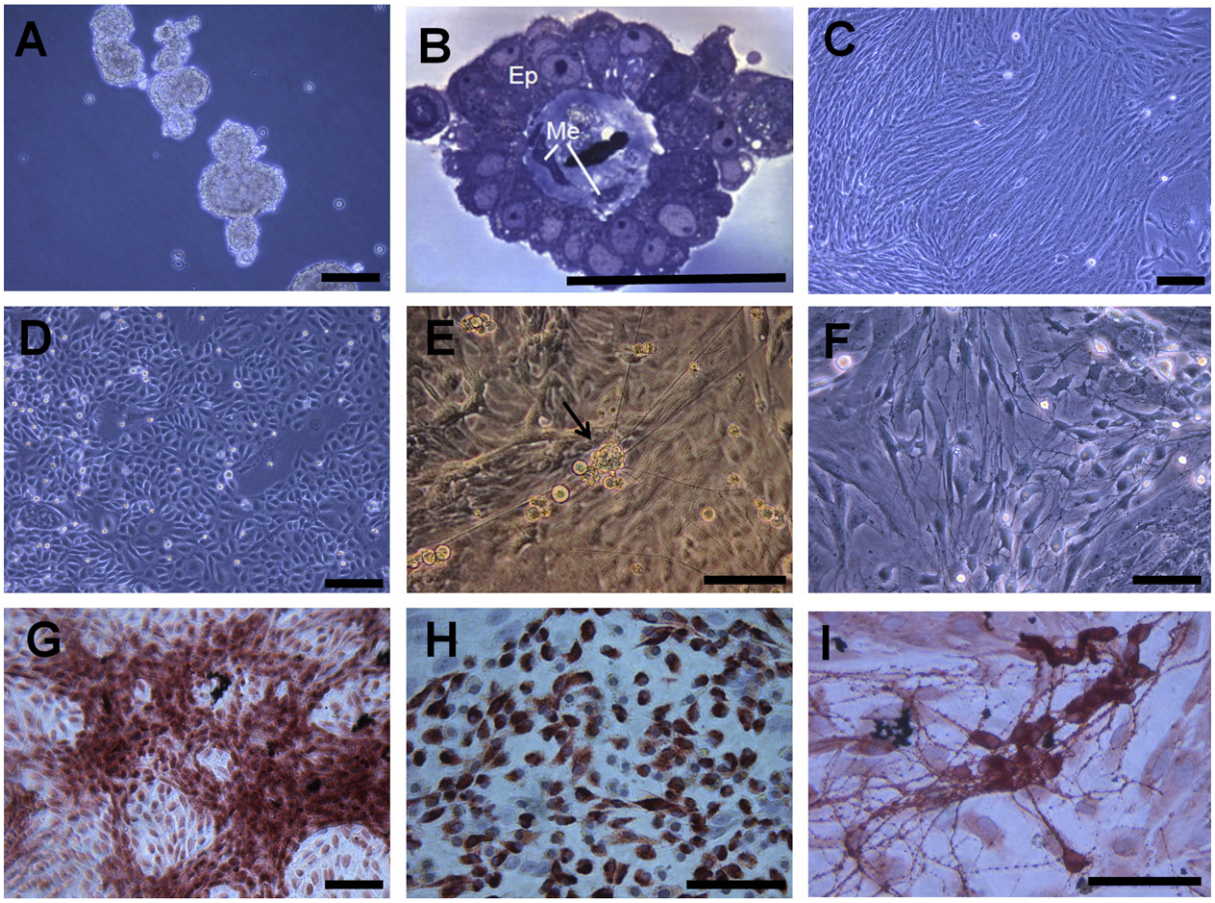

Figure 4 In vitro differentiation of porcine EGC. (A) Embryoid bodies. (B) Light micrograph of embryoid body derived from putative EGC. Note the outer layer of endodermal-like epithelium (Ep) surrounding mesenchymal cells (Me) embedded in extracellular matrix. (C) Mesenchymal-like cells. (D) Epithelial-like cells. (E) Neuronal-like cells (arrow) growing on the surface of other cells. (F) Neuronal-like cells embedded in the cell layer. (G) Epithelial-like cells stained for Fox2A. (H) Mesenchymal-like cells stained for vimentin. (I) Neuronal-like cells stained for Tuj1 (all scale bars = 50 μm).

mice, 3/9 mice developed single, clearly defined tumors in the neck (Figs. 5A and C), and in one instance a small tumor formed in the back area. All three mice injected intramuscularly developed multiple outgrowths per injection site (Figs. 5B and D). None of the negative control mice (without injections, injected with PBS, with STO feeder cells, or differentiated putative EGC) developed any tumors.

Analysis of the stained paraffin sections showed that the major central portion of the tumors consisted of a homogeneous, rather undifferentiated cell population with few tubular structures lined with cuboidal or columnar epithelium (Figs. 5E and F) located mostly in the periphery. When the species origin of the tumors was tested by PCR using porcine-specific GAPDH primers, there was no amplification from the tumor samples (Fig. S3A). Restriction digestion of the GAPDH amplification products confirmed that the tumors consisted of mouse cells (data not shown). Microsatellite analysis showed the presence of both STO feeders and NMRI-nude host cells in all tumors (Fig. S3B and Table S3).

Discussion

Based on our current knowledge on PGC specification, migration, and differentiation, we reasoned that it might be beneficial to culture PGC from earlier developmental stages than reported before in order to obtain porcine pluripotent cells. In our hands, PGC from Day 20–24 embryos proliferated robustly and this enabled us to establish cell lines from individual embryos with high efficiency. In comparison, other research groups have used pooled PGC from entire litters, and the authors have, despite this, reported low efficiency of putative EGC line derivation (Shim et al., 1997; Tsung et al., 2003). Furthermore, this is the first report of culture of PGC from the Yucatan mini pig, a breed of importance as a biomedical model of human disease as well as potential source of organs for xenotransplantation.

In contrast to the successful culture of PGC at Days 20–24, we were not able to culture these cells from the hindguts of embryos at Days 17–18 of gestation in the long term. A possible explanation for these results is that the culture conditions currently used are only suitable for culture of PGC from the mesonephic-genital ridge area (Day 20+), and that cells at stages that are closer to epiblast (before Day 20) fail to proliferate in the long term, or differentiate, similar to cultured pig ICM or epiblast cells. In future studies, different conditions will need to be tested in order to optimize the culture of PGC from earlier stages.

The putative EGC were identified in culture by their strong AP activity and expression of SSEA4, TRA-1-61, TRA-1-80, and C-KIT (in primary cultures; Fig. 3). Alkaline phosphatase is commonly used as a marker for identification of murine PGC (Ginsburg et al., 1990), and in the area of hindgut-mesentery-mesonephros-genital ridge it is

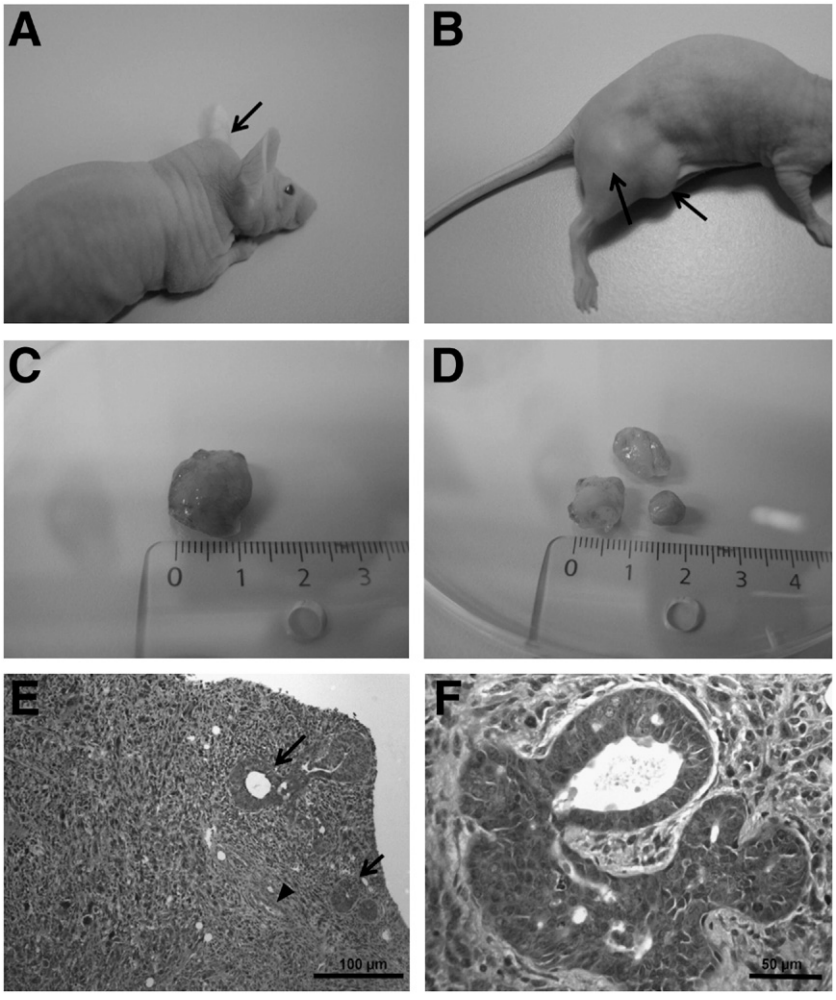

Figure 5 Tumor formation in NMRI-nude mice. (A) Neck tumor (arrow). (B) Multiple hind-leg tumors (arrows). (C) Isolated neck tumor (ruler format is in cm). (D) Isolated hind-leg tumors (ruler format is in cm). (E) Paraffin section of neck tumor stained with hematoxylin-eosin showing peripherally located tubular structures with cuboidal (arrowhead) and columnar (arrows) epithelium (scale bar = 100 μm). (F) High magnification photograph of a tubular structure with columnar epithelium (scale bar = 50 μm).

restricted to the germ line, as shown for the stages corresponding to porcine Days 20–25 in the bovine (Wrobel and Süß, 1998) and ovine (Ledda et al., 2010) species. Of the remaining markers, SSEA4, TRA-1-61, and TRA-1-80 are expressed in human PGC and EGC (Shamblott et al., 1998), as well as in porcine EGC isolated from genital ridges (Tsung et al., 2003; Petkov and Anderson, 2008). Additionally, the colony morphology of our putative EGC was identical with porcine EGC derived from genital ridges described in previous reports (Tsung et al., 2003; Petkov and Anderson, 2008), further confirming the germ-line character of the cultured cells.

Electron microscopy revealed that the putative EGC are connected with intermediate and tight junctions, which may explain the difficulty in disaggregating the colonies. Additionally, we found that the cells possess cilia on their surfaces. It has been shown that cilia are an important component of cell signaling mechanisms and are present in certain cell types, including human ESC, where they play an important role in differentiation by harboring components of the Hedgehog signaling pathway (Kiprilov et al., 2008).

A number of our PGC-derived cell lines were characterized for expression of pluripotency markers using a wide range of methods, such as immunocytochemistry, RT-PCR, and, for the first time, RNA-Seq analysis (the data obtained from the latter is available as a resource for other studies at GEO GSE24220). The expression of key pluripotency genes such as *OCT4*, *SOX2*, and *NANOG* was not detected at the transcriptional and protein level, suggesting that the cells are not pluripotent. The absence of *OCT4* expression is confounding, since this gene is expressed in mouse and human EGC. A possible explanation is that the expression of OCT4 is rapidly lost in culture due to changes occurring in the cells under the culture conditions. This hypothesis is supported by the surprisingly fast downregulation of *C-KIT* and *TDH* expression. On the other hand, we cannot speculate on the absence of NANOG and SOX2, because currently data on the expression of these genes in pig PGC are not available. It has been shown that SOX2 is not expressed in human germ cells and EGC (Perrett et al., 2008), which suggests that this gene may have different role in the germ-line development in the nonmurine species.

On the other hand, the stem cell-like character of the cells was confirmed by expression of other pluripotency-related genes at levels comparable to those in murine ESC, such as *FBXO15*, *ID2*, *C-MYC*, *KLF4*, and *CHD1*. The relevance of *CHD1* is that this gene is involved in maintaining an open chromatin configuration and is important for maintenance of pluripotency of murine ESC (Gaspar-Maia et al., 2009). Additionally, we detected protein expression of AP, SSEA-4, TRA-1-60, and TRA-1-81 by immunostaining. These findings suggest that the putative EGC have preserved some pluripotency characteristics. Interestingly, the RNA-Seq data showed that a few pluripotency genes were expressed at significantly higher levels in pFF, such as *SOX2*. However, one of the reasons that *SOX2* is present in the pFF might be that, next to being pivotal for pluripotency, this gene also has a role in neuronal differentiation (Kishi et al., 2000). The expression of pluripotency-specific genes by the pFF further suggests that these might not be completely differentiated into any of the somatic lineages. This is supported by reports where cells isolated from fetal porcine skin possess a certain level of "stemness" and are able to differentiate into germ-like cells (Dice et al., 2006) and neural progenitors (Zhao et al., 2010). Moreover, fetal fibroblasts from mouse and sheep embryos have contributed to somatic chimeras when injected into blastocysts (Karasiewicz et al., 2008; Piliszek et al., 2007). In comparison with the murine ESC, our putative pig EGC showed an expression pattern slightly directed toward the endo/mesodermal lineage unlike the pFF, which show strong ectodermal differentiation. The differences between these two cell types are further underlined by functional (PANTHER) analysis, which shows that the differentially expressed genes in pFF are associated with mesodermal, endodermal, skeletal, and other developmental processes.

The expression of germ-line-specific genes was also detected in the putative EGC, showing a consistent increase compared with pFF. All of our analyzed PGC-derived cell lines expressed *BLIMP1* during the entire period of culture (over 10 passages), even in the presence of bFGF at concentrations as high as 10 ng/ml (data not shown). Interestingly, BLIMP1 did not downregulate the expression of *c-myc* and *Klf4* in our porcine PGC-derived cell lines. As this downregulation is observed in mouse, it suggests a slightly different mode of action of BLIMP1 in the porcine species as compared with mouse. One possible explanation for this difference is the cytoplasmic localization of this gene in our putative EGC. It has been shown in mouse PGC that prior to their arrival in the genital ridges Blimp1 is localized in the nucleus but translocates to the cytoplasm afterward, thereby losing its function as a transcriptional repressor (Ancelin et al., 2006). It is therefore possible that the porcine PGC have continued their germ-line differentiation program in vitro, characterized by the loss of nuclear BLIMP1 localization and associated with it *MYC* and *KLF4* repression.

Elements of the LIF signaling pathway, namely *LIFr*, *gp130*, and *STAT3*, were detected in all of the tested cell lines. Similarly, we detected transcripts for FGF receptors 1 and 2. This suggests that these pathways may be active in porcine PGC; however, as the use of hrLIF and hrbFGF apparently did not facilitate the isolation of pluripotent cells, additional factors might be required to maintain pluripotency in porcine EGC. On the contrary, the use of hrSCF can be questioned since the expression of *C-KIT* was absent after P0 in all of the tested cell lines.

Finally, *TDH* was shown to be expressed in our putative EGC lines at P0, but was not detected at P3 (data not shown) or P6–7. A recent publication (Wang et al., 2009) showed that mouse ESC and embryos are critically dependent on threonine and on the function of the *Tdh* gene for their fast proliferation. Therefore, the downregulation of TDH may explain the typical slow proliferation of porcine putative EGC.

Porcine EGC have been reported by us and other groups to be capable of forming simple EB (Piedrahita et al., 1998; Shim et al., 1997; Tsung et al., 2003; Petkov and Anderson, 2008). In our hands, the putative EGC derived from younger embryos formed EB-like aggregates that were indistinguishable from those pictured in these reports. Characteristically, these aggregates have a simple structure and differ from mouse and human EB, which are larger and contain multiple differentiated cell types. When allowed to attach on gelatin-treated plastic surfaces, they proliferated extensively and formed different cell types, such as epithelial-like, mesenchymal-like, and neuronal-like cells. It should be noted, however, that the differentiation was limited in scope, and cells in a more advanced stage of differentiation (such as beating cardiac muscle cells) were not observed, despite the adaptation of differentiation protocols applied in mouse and human ESC differentiation (results not shown).

When injected in immunodeficient mice, ESC form teratomas that contain differentiated cells from the three germ layers. In contrast, injection of our putative porcine EGC into nude mice did not result in teratoma formation. Interestingly, human EGC usually fail to form teratomas when injected as undifferentiated cell population (Shamblott et al., 2000; Turnpenny et al., 2005); however, EB-derived cells resulting from in vitro differentiation of human EGC have been able to differentiate into neurons and glia (Teng et al., 2009) and liver cells (Chen et al., 2007) when injected into the brain or liver of immunodeficient mice. The reasons for this discrepancy are not currently known.

As a result of our injections, the experimental mice developed tumors that clearly show the presence of STO feeders together with the host mouse cells. This is in agreement with a report where tumors of mouse origin have formed as a result of ovine EGC injection (Ledda et al., 2010). One possible explanation for our results would be that the feeder cells were not completely inactivated by the mitomycin C treatment. However, our control assessments of the mitotic inactivation of the mitomycin C-treated feeder cells before and after the injection experiments have indicated that they do not proliferate in culture. Moreover, injection of up to 2×10^6 STO cells alone did not result in tumor formation within 14 weeks after injection. This may suggest that even though

the injected porcine cells did not form teratomas, they might have influenced the proliferation of the neighboring STO and/or host cells. Taking into account that even a small fraction of mitomycin C-treated feeder cells may contribute to tumor formation, complete removal of the feeder cells may be necessary when injecting cells for teratoma analysis. In addition, our experience obviates the need for verification of the species origin of the teratomas, especially if the tested cells have been cultured on feeder layers.

In conclusion, we isolated putative porcine EGC from PGC with high efficiency using embryos from domestic breeds and Yucatan mini pig at Days 20–24 of gestation. We applied for the first time genome-wide RNA-Seq expression profiling in the porcine species to show that the resulting cell lines are not pluripotent, but rather possess multipotent characteristics, potentially due to their retained germ-line specification. This observation is further supported by the immunostainings, the differentiation assays, and the cell's inability to form teratomas. Further culture conditions must be tested for obtaining the pluripotent counterparts of the putative EGC described in this study. The observations made in this study, such as the activity of various signaling pathways present in porcine which are important for pluripotency in other species, will however be of critical importance to determine the optimal supplementary factors for culturing these cells.

Materials and methods

All chemicals were purchased from Sigma-Aldrich (Saint Louis, MO, USA), unless indicated otherwise.

Experimental animals

The housing and breeding of the pigs used for embryo production complied with the Danish Animal Welfare Act (1991), The Act on Housing of Pregnant Sows and Gilts (1999), as well as the EU Directive 91/630/EEC. The mice were housed and treated according the Danish law on animal experimentation. All teratoma studies were undertaken with prior approval from the Danish Council for Animal Experimentation (2006/561-1125-C2).

Primordial germ cell collection and culture

Danish Landrace sows were artificially inseminated with semen from Yorkshire boars 4–5 days after weaning of their litters and sacrificed at Days 17–18, 20–21, 22–23, or 23–24 of pregnancy. One Yucatan mini pig sow was bred with boar from the same breed and collected at Days 23–24 of pregnancy. The primary culture of PGC was performed as described in (Petkov and Anderson, 2008). Briefly, hindguts were isolated from Day 17 to 18 embryos, while the medial parts of the mesonephros, including the areas of genital ridge formation, were dissected from the later stages. The tissues were disaggregated by trypsinization, and the cell suspensions were cultured on mouse STO feeder layers with EGC culture medium (AQ Media supplemented with 17% KSR, nonessential amino acids, penicillin-streptomycin, 10 ng/ml human recombinant LIF (Millipore, Billerica, USA), 10 ng/ml human recombinant SCF (Prospec, Rehovot, Israel), and 3 ng/ml human recombinant bFGF (Invitrogen, Carlsbad, USA)). For the first passage (P1) the primary culture colonies were purified from the somatic and feeder cells by disaggregation of the cultures with 1 mg/ml Collagenase IV for 10 min at 37 °C and filtering of the suspensions three times through 23-μm polyester mesh (Spectrum Labs, Los Angeles, USA). The putative EGC colonies (which are very tightly packed and could not be disaggregated by Collagenase IV treatment) were recovered by washing the mesh with PBS, disaggregated by trypsinization, and then split onto fresh feeders. At the second and all later passages the putative EGC colonies were split together with the feeder cells by trypsin disaggregation at ratios 1:2–1:3 every 4–5 days.

Culture of porcine fetal fibroblasts

After hindgut/mesonephros dissection for PGC isolation, the heads and the remaining internal organs were removed, and the embryos were further fragmented, trypsinized for 15 min, and disaggregated by pipetting, and the cell suspensions were cultured in 75 cm^2 flasks with AQ media supplemented with 15% FBS and penicillin-streptomycin.

Transmission and scanning electron microscopy

Putative EGC colonies at different passages were fixed in 3% glutaraldehyde in 0.1 M sodium phosphate buffer, pH 7.2–7.4, at 4 °C for 1 h, washed twice in 0.1 M sodium phosphate buffer, postfixed in 1% OsO_4 in 0.1 M sodium phosphate buffer for 1 h at 4 °C, and washed in 0.1 M sodium phosphate buffer. The samples for transmission electron microscopy (TEM; EGC colonies at passage 4) were dehydrated in a graded ethanol series, embedded in Epon using propylene oxide as an intermediate, and serially sectioned into semithin sections (2 μm), which were stained with toluidine blue for light microscopy (LM). Selected semithin sections were subsequently trembedded (Hyttel and Madsen, 1987), and ultrathin sections were prepared. The ultrathin sections were collected on copper grids, contrasted with uranyl acetate and lead citrate, and examined on a Philips CM 100 transmission electron microscope. The samples for scanning electron microscopy (SEM; EGC colonies at passages 4, 8, and 9) were dehydrated in a graded acetone series, critical-point-dried (EMS 850 Critical Point Drier (Electron Microscopy Sciences, Hatfield, PA, USA)), sputter-coated with gold–palladium SC7640 Suto/Manual High Resolution Sputter Coater (Quorum Technologies, Newhaven, UK), and examined in a Jeol scanning electron microscope (FEI Quanta 200 (FEI Company, Eindhoven, The Netherlands)).

Gene expression analysis by RT-PCR

For RT-PCR analysis primary EGC colonies (P0) as well as EGC colonies at P3–8 were purified by Collagenase IV treatment and triple filtration as described above. Total RNA was extracted using an RNeasy Mini Kit (Qiagen, Hilden, Germany), and reverse transcription was performed using RevertAid reverse transcriptase (Fermentas, Burlington, Canada) according to the manufacturer's instructions, using oligo $T_{(18)}$VN primer. PCR was performed on 50 ng reverse-transcribed total RNA/reaction using custom-designed primers (supplementary Table S1). We ensured that the selected primers did not produce PCR products from mouse STO cell cDNA.

Gene expression analysis by RNA-Seq

Total RNA was isolated using Trizol (Invitrogen) according to the manufacturer's recommendations. One hundred micrograms of total RNA was subjected to two rounds of poly(A) selection (Oligotex mRNA Mini Kit; Qiagen), followed by DNaseI treatment (Qiagen). The amounts of 100–200 ng mRNA were fragmented by hydrolysis (5X fragmentation buffer: 200 mM Tris acetate, pH 8.2, 500 mM potassium acetate, and 150 mM magnesium acetate) at 94 °C for 90 s and purified (RNAeasy Minelute Kit; Qiagen). cDNA was synthesized using 5 μg random hexamers by Superscript III Reverse Transcriptase (Invitrogen). Ds-cDNA synthesis was performed in second-strand buffer (Invitrogen) according to the manufacturer's recommendations and purified (Minelute Reaction Cleanup Kit; Qiagen). Quality control was performed by qPCR.

Ds-cDNA samples were prepared for sequencing by end repair of 20 ng DNA as measured by Qubit (Invitrogen). Adaptors were ligated to DNA fragments, followed by size selection (~300 bp) and limited PCR amplification (14 cycles). Quality control was performed by qPCR and by running the products on a Bioanalyzer (BioRad). Cluster generation and sequencing-by-synthesis (36 bp) were performed using the Illumina Genome Analyzer IIx (GAIIx) platform according to standard protocols (Illumina). Samples were sequenced to a depth of approximately 15 million mapped tags per sample. Sequences were aligned to the pig SGSC Sscrofa9.2/susScr2 reference genome using the Illumina Analysis Pipeline allowing one mismatch. Only the tags uniquely aligning to the genome were considered for further analysis. Further analysis was performed using the 36-bp sequence reads. The output data were converted to Browser Extensible Data (BED) files for downstream analysis and Wiggle (WIG) files for viewing. All sequencing analyses were conducted based on the *Sus scrofa* SGSC Sscrofa9.2/susScr2 genome assembly accessed from the UCSC Genome Browser (assembly November 2009). All RNA-Seq data (FASTQ, BED, and WIG files) are present in the NCBI GEO SuperSeries GSE24220.

Quantification of RNA-Seq

Gene annotation was retrieved from Biomart (http://www.biomart.org) using Ensembl Genes (Ensembl Genes 59 (Sanger UK), Sscrofa9). Orthology information was also retrieved from Biomart. To obtain gene expression values from the RNA-Seq output, we counted the number of tags present in the coding bodies of genes. The gene expression values were converted to standardized RNA-Seq expression values "Reads Per Kilobase exon Model per million mapped read" (RPKM) (Mortazav et al., 2008). The selection of lineage specific genes and pluripotency markers was obtained from (Mikkelsen et al., 2007). GO, KEGG and PANTHER analysis was performed using DAVID (Huang Test, 2009). Gene ontology of *Sus scrofa* is very poor, and therefore insufficient to perform genome-wide functional studies in its current state for the pig. Thus, all DAVID analysis was performed using mouse background.

Alkaline phosphatase staining

Alkaline phosphatase staining was performed with 5-bromo-4-chloro-3-indolyl phosphate (100 μg/ml) and nitroblue tetrazolium (500 μg/ml) in 100 mM Tris buffer (pH 8.5) supplemented with 100 mM NaCl and 50 mM $MgCl_2$.

Immunocytochemistry

All procedures were performed at room temperature, unless indicated otherwise. For immunostaining, the cultures were fixed with 4% paraformaldehyde for 15 min. For all nuclear-localized antigens, the cells were permeabilized in 0.5% Triton X for 15 min followed by antigen demasking by 3×5 min incubations in boiling citrate buffer (10 mM citric acid, 0.05% Tween 20, pH 6.0). Nonspecific antibody binding was blocked with 2% bovine serum albumin in PBS for 1 h. Endogenous peroxidase activity was blocked by treatment with 0.03% hydrogen peroxide for 5 min. Primary antibodies used were OCT4 (Santa Cruz Biotechnology, Santa Cruz, USA; 1:500), SOX2 (R&D Systems, Minneapolis, USA; 1:200), NANOG (Chemicon International, Temecula, USA; 1:800), BLIMP1 (Novus Biologicals, Denver, USA; 1:500), SSEA-1 (BioLegend, San Diego, USA; 1:300), SSEA-4 (BioLegend; 1:500), C-MYC (Abcam, Cambridge, UKl 1:300), TRA-1-60 (BioLegend; 1:300), and TRA-1-81 (BioLegend; 1:300), during incubation for 1 h on a shaking platform. Nonbound antibody was washed away with PBS and bound antibody was visualized using EnVision+System with peroxidase (DAB) (DAKO, North Aurora, USA), according to the manufacturer's instructions.

The EB outgrowths were stained with antibodies against cytokeratin (Abcam), Fox2A (Abcam), vimentin (Zymed Labs, San Francisco, USA), and beta III tubulin (Covance, Emeryville, USA), all applied at dilutions 1:500, and visualized as described above.

In vitro differentiation

For embryoid body (EB) formation purified putative EGC colonies were disaggregated to single cells by trypsinization and incubated in "hanging drops" in AQ medium supplemented with 15% FBS at density 2000 cells/25 μl drop for 5–7 days. For further differentiation, the EB were plated on gelatin-treated plastic dishes for 10–14 days.

Teratoma formation and analysis

For teratoma formation, mouse STO feeders were depleted from porcine EGC by filtration as described above and cells from 5 Landrace and 5 Yucatan mini pig EGC lines at passages 7–9 were injected as single cell suspensions subcutaneously in the neck and back areas of NMRI-nude mice (NMRINU-M, Taconic, Bomholt, Denmark). All injections were performed on anesthetized mice. At least one injection of $1.8–2\times10^6$ cells was performed for each line, and additional injections of $1–5\times10^6$ cells were performed for six of the tested EGC lines. In addition, three mice were injected intramuscularly in the hind leg with $3–5\times10^6$ single cells or whole EGC colonies. As negative controls mice were kept without injections, or injected either with injection solution (PBS), 2×10^6 mitomycin C-inactivated feeder cells, or 2×10^6 differentiated EGC (maintained as monolayers without feeders and growth factors for several passages). The mice were kept in cages under sterile laminar flow conditions and monitored each day for a maximum period of 14 weeks.

Dissected tumor outgrowths were partitioned and either fixed in 4% paraformaldehyde for paraffin-embedding or fixed in formalin buffer, pH 7.0 (Lilly´s fixative, Bie&Bernstein A/S, Roedovre, Denmark), followed by cryoprotection for freeze embedding in Tissue tek (Sakura Finetek Europe, Zoeterwoude, The Netherlands). Paraffin-embedded sections and cryosections were stained with hematoxylin and eosin for morphological assessment.

For PCR analysis, DNA was extracted from tumors, cultured STO cells, and nude mouse tail using a DNeasy Blood Kit (Qiagen) according to the manufacturer's protocol. For determination of the species origin, GAPDH was amplified by PCR using porcine-specific (Table S1) and universal primers (Fermentas) as described above. To determine the species origin of the tumor samples, the PCR products from the universal primers were digested using SacI restriction enzyme (Fermentas), which has restriction site only within the porcine sequence. Microsatellite analysis by PCR was performed with primers adapted from (Saha, 1996) (microsatellite 1) and (Zhang et al., 2005) (microsatellite 2). The reverse primers from each pair were labeled with either FAM or HEX, and the PCR were performed using the conditions described earlier, followed by capillary electrophoresis using ABI Prism 3130xl Genetic Analyzer (Applied Biosystems).

Supplementary materials related to this article can be found online at doi:10.1016/j.scr.2011.01.003.

Acknowledgments

We thank Kees-Jan Françoijs, Simon van Heeringen, and Eva Janssen-Megens for help with sequencing and sequence analysis. In addition, we thank the management of Tisbaek farm for the insemination and care of the pregnant animals, Dr. Jacob Bentzon

for the breeding and care of the pregnant Yucatan mini pig sow, and Dr. Merete Fredholm for her help with the capillary sequencing of the microsatellite PCR samples. This study was supported by EU FP7 Stem Cell Projects "PartnErS" (218205;204,523) and "PluriSys" (223485) as well as the National Advanced Technology Foundation Project "Pigs and Health."

References

Ancelin, K., Lange, U., Hajkova, P., Schneider, R., Bannister, A., Kouzarides, T., Surani, A., 2006. Blimp1 associates with Prmt5 and directs histone arginine methylation in mouse germ cells. Nat. Cell Biol. 8 (6), 623–630.

Brevini, T., Antonini, S., Pennarossa, G., Gandolfi, F., 2008. Recent progress in embryonic stem cell research and its application in domestic species. Reprod. Dom. Anim. 43 (Suppl. 2), 193–199.

Buehr, M., 1997. The primordial germ cells of mammals: Some current perspectives. Exp. Cell Res. 232 (2), 194–207.

Chen, B., Shi, J., Zheng, J., Chen, Y., Wang, K., Yang, Q., Chen, X., Yang, Z., Zhou, X., Zhu, Y., Chu, J., Liu, A., Sheng, H., 2007. Differentiation of liver cells from human primordial germ cell-derived progenitors. Differentiation 75, 350–359.

Dice, P.W., Wen, L., Li, J., 2006. In vitro germline potential of stem cells derived from fetal porcine skin. Nat. Cell Biol. 8 (4), 384–390.

Durcova-Hills, G., Tokunaga, T., Kurosaka, S., Yamaguchi, M., Takashi, S., Imai, H., 1999. Immunomagnetic isolation of primordial germ cells and the establishment of embryonic germ cell lines in the mouse. Cloning 1, 217–224.

Durcova-Hills, G., Ainscouth, J., McLaren, A., 2001. Pluripotent stem cells derived from migrating primordial germ cells. Differentiation 68 (4–5), 220–226.

Durcova-Hills, G., Burgoyne, P., McLaren, A., 2004. Analysis of sex differences in EGC imprinting. Dev. Biol. 268 (1), 105–110.

Durcova-Hills, G., Adams, I., Barton, S., Surani, A., McLarren, A., 2006. The role of exogenous fibroblast growth factor-2 on the reprogramming of primordial germ cells into pluripotent stem cells. Stem Cells 24, 1441–1449.

Durcova-Hills, G., Tang, F., Doody, G., Tooze, R., Surani, A., 2008. Reprogramming primordial germ cells into pluripotent stem cells. PLoS ONE 3 (10), e3531.

Gaspar-Maia, A., Alajem, A., Polesso, F., Sridharan, R., Mason, M., Heidersbach, A., Ramalho-Santos, J., McManus, M., Plath, K., Meshorer, E., Ramalho-Santos, M., 2009. Chd1 regulates open chromatin and pluripotency of embryonic stem cells. Nature 460 (7257), 863–868.

Ginsburg, M., Snow, M., McLaren, A., 1990. Primordial germ cells in the mouse embryo during gastrulation. Development 110, 521–528.

Hall, V., 2008. Porcine embryonic stem cells: a possible source for cell replacement therapy. Stem Cell Rev. 4 (4), 275–282.

Hayashi, K., Chuva de Sousa Lopes, S., Surani, A., 2007. Germ cell specification in mouse. Science 316 (5823), 394–396.

Huang Test, W., 2009. Systematic and integrative analysis of large gene lists using DAVID bioinformatics resources. Nat. Protoc. 4, 44–57.

Hyttel, P., Madsen, I., 1987. Rapid method to prepare mammalian oocytes and embryos for transmission electron microscopy. Acta Anat. 129, 12–14.

Karasiewicz, J., Sacharczuk, M., Was, B., Guszkiewicz, A., Korwin-Kossakowski, M., Gorniewska, M., Szablisty, E., Modlinski, J.A., 2008. Experimental embryonic-somatic chimaerism in the sheep confirmed by random amplified polymorphic DNA assay. J. Int. Dev. Biol. 52, 315–322.

Keefer, C., Panta, D., Blomberg, L., Talbot, N., 2007. Challenges and prospects for the establishment of embryonic stem cell lines of domesticated ungulates. Anim. Reprod. Sci. 98, 147–168.

Kiprilov, E., Awan, A., Desprat, R., Velho, M., Clement, C., Byskov, A., Andersen, C., Satir, P., Bouhassira, E., Christensen, S., Hirsch, R., 2008. Human embryonic stem cells in culture possess primary cilia with hedgehog signaling machinery. J. Cell Biol. 180 (5), 897–904.

Kishi, M., Miyuseki, K., Sasai, N., Yamazaki, H., Shiota, K., Nakanishi, S., Sasai, Y., 2000. Requirement of Sox2-mediated signaling for differentiation of early Xenopus neuroectoderm. Development 127, 791–800.

Labosky, P., Barlow, D., Hogan, B., 1994. Mouse embryonic germ (EG) cell lines: transmission through the germ line and differences in the methylation imprint of insulin-like growth factor 2 receptor (Igf2r) gene compared with embryonic stem (ES) cell lines. Development 120 (11), 3197–3204.

Ledda, S., Bogliolo, L., Bebbere, D., Ariu, F., Pirino, S., 2010. Characterization, isolation and culture of primordial germ cells in domestic animals: recent progress and insights from the ovine species. Theriogenology 74, 534–543.

Matsui, Y., Zsebo, K., Hogan, B., 1992. Derivation of pluripotential embryonic stem cells from murine primordial germ cells in culture. Cell 70 (5), 841–847.

Mikkelsen, T., Ku, M., Jaffe, D., Issac, B., Lieberman, E., Giannoukos, G., Alvarez, P., Brockman, W., Kim, T., Koche, R., Lee, W., Mendenhall, E., O'Donovan, A., Presser, A., Russ, C., Xie, X., Meissner, A., Wernig, M., Jaenisch, R., Nusbaum, C., Lander, E., Bernstein, B., 2007. Genome-wide maps of chromatin state in pluripotent and lineage-committed cells. Nature 448, 553–560.

Mortazav, A., Williams, B., McCue, K., Schaeffer, L., Wold, B., 2008. Mapping and quantifying mammalian transcriptomes by RNA-Seq. Nat. Meth. 5, 621–628.

Müller, S., Prelle, K., Rieger, N., Petznek, H., Lassnig, C., Luksch, U., Aigner, B., Baetscher, M., Wolf, E., Mueller, M., Brem, G., 1999. Chimeric pigs following blastocyst injection of transgenic porcine primordial germ cells. Mol. Reprod. Dev. 54 (3), 244–254.

Ohinata, Y., Payer, B., O'Carrol, D., Ancelin, K., Ono, Y., Sano, M., Barton, S., Obukhanych, T., Nussenzweig, M., Tarakhovsky, A., Saitou, M., Surani, A., 2005. Blimp1 is a critical determinant of the germ cell lineage in mice. Nature 436, 207–213.

Okita, K., Ichisaka, T., Yamanaka, S., 2007. Generation of germ line-competent induced pluripotent stem cells. Nature 448, 313–317.

Perrett, R., Turnpenny, L., Eckert, J., O'Shea, M., Sonne, S., Cameron, I., Wilson, D., Rajpert-De Meyts, E., Hanley, N., 2008. The early human germ cell lineage does not express SOX2 during In vivo development or upon In vitro culture. Biol. Reprod. 78, 852–858.

Pesce, M., Farrace, M., Piacentini, M., Dolci, S., Felici, M., 1993. Stem cell factor and leukemia inhibitory factor promote primordial germ cell survival by suppressing programmed cell death (apoptosis). Development 118 (4), 1089–1094.

Petkov, S., Anderson, G., 2008. Culture of porcine embryonic germ cells in serum-supplemented and serum-free conditions: the effects of serum and growth factors on primary and long-term culture. Cloning Stem Cells 10 (2), 263–276.

Piedrahita, J., Moore, C., Oetama, B., Lee, C.-K., Scales, N., Jagdeece, R., Bazer, F., Ott, T., 1998. Generation of transgenic porcine chimeras using primordial germ cell-derived colonies. Biol. Reprod. 58 (5), 1321–1329.

Piliszek, A., Modlinski, J.A., Pysniak, K., Karasiewicz, J., 2007. Foetal fibroblasts introduced to cleaving mouse embryos contribute to full-term development. Reproduction 133, 207–218.

Resnick, J., Bixler, L., Cheng, L., Donovan, P., 1992. Long-term proliferation of mouse primordial germ cells in culture. Nature 359 (6395), 550–551.

Saha, B., 1996. Typing of murine major histocompatibility complex with a microsatellite in the class II *Eb* gene. J. Immunol. Meth. 194, 77–83.

Saitou, M., Payer, B., O'Carroll, D., Ohinata, Y., Surani, A., 2005. Blimp1 and the emergence of the germ line during development in the mouse. Cell Cycle 4 (12), 1736–1740.

Sette, C., Dolci, S., Geremia, R., Rossi, P., 2004. The role of stem cell factor and of alternative c-kit gene products in the establishment, maintenance and function of germ cells. Int. J. Dev. Biol. 44 (6), 599–608.

Shamblott, M., Axelman, J., Wang, S., Bugg, E., Littlefield, J., Donovan, P., Blumenthal, P., Huggins, G., Gearhart, J., 1998. Derivation of pluripotent stem cells from cultured human primordial germ cells. Proc. Natl Acad. Sci. USA 95, 13726–13731.

Shamblott, M., Axelman, J., Littlefield, J., Blumenthal, P., Huggins, G., Cui, Y., Cheng, L., Gearhart, J., 2000. Human embryonic germ cell derivatives express a broad range of developmentally distinct markers and proliferate extensively in vitro. Proc. Natl Acad. Sci. USA 98, 113–118.

Shim, H., Gutiérres-Adán, A., Chen, L.-R., BonDurant, R., Behboodi, E., Anderson, G., 1997. Isolation of pluripotent stem cells from cultured porcine primordial germ cells. Biol. Reprod. 57 (5), 1089–1095.

Shim, S., Han, D., Yang, J., Lee, B., Kim, S., Shim, H., Lee, H., 2008. Derivation of embryonic germ cells from post migratory primordial germ cells, and methylation analysis of their imprinted genes by bisulfite genomic sequencing. Mol. Cells 25 (3), 358–367.

Stewart, C., Gadi, I., Bhatt, H., 1994. Stem cells from primordial germ cells can reenter the germ line. Dev. Biol. 161 (2), 626–628.

Tada, T., Tada, M., Hilton, K., Barton, S., Sado, T., Takagi, N., Surani, A., 1998. Epigenotype switching of imprintable loci in embryonic germ cells. Dev. Genes Evol. 207 (8), 551–561.

Takashi, K., Yamanaka, S., 2006. Induction of pluripotent stem cells from mouse embryonic and adult fibroblast cultures by defined factors. Cell 126, 663–676.

Takashi, K., Tanabe, K., Ohnuki, M., Narita, M., Ichisaka, T., Tomoda, K., Yamanaka, S., 2007. Induction of pluripotent stem cells from adult human fibroblasts by defined factors. Cell 131, 861–872.

Teng, Y., Chen, B., Tao, M., 2009. Human primordial germ cell-derived progenitors give rise to neurons and glia in vivo. Biochem. Biophys. Res. Commun. 390 (3), 463–468.

Tsung, H., Du, Z., Rui, R., Li, X., Bao, L., Wu, J., Bao, S., Yao, Z., 2003. The culture and establishment of embryonic germ (EG) cell lines from Chinese mini swine. Cell Res. 13 (3), 195–202.

Turnpenny, L., Cameron, I., Spalluto, C., Hanley, K., Wilson, D., Hanley, N., 2005. Human embryonic germ cells for future neuronal replacement therapy. Brain Res. Bull. 68, 76–82.

Uenishi, H., Eguchi, T., Suzuki, K., Sawazaki, T., Toki, D., Shinkai, H., Okumura, N., Hamasima, N., Awata, T., 2004. PEDE (Pig EST Data Explorer): construction of a database for ESTs derived from porcine full-length cDNA libraries. Nucleic Acids Res. 32, D484–D488.

Vaskova, I., Ungrova, A., Lopes, F., 2007. Putative embryonic stem cell lines from pig embryos. J. Reprod. Dev. 53, 1137–1149.

Wang, J., Alexander, P., Wu, L., Hammer, R., Cleaver, O., McNight, S., 2009. Dependence of mouse embryonic stem cells on threonine catabolism. Science 325 (5939), 435–439.

Wrobel, K.-H., Süß, F., 1998. Identification and temporospatial distribution of bovine primordial germ cells prior to gonadal sexual differentiation. Anat. Embryol. 197, 451–467.

Zhang, M., Joseph, B., Gupta, S., Guest, I., Xu, M., Sell, S., Son, K., Koch, K., Leffert, H., 2005. Embryonic mouse STO cell-derived xenografts express hepatocytic functions in the livers of nonimmunosupressed adult rats. Stem Cells 23, 186–199.

Zhao, M.T., Whitworth, K.M., Lin, H., Zhang, X., Isom, S.C., Dobbs, K.B., Bauer, B., Zhang, Y., Prather, R.S., 2010. Porcine skin-derived progenitor (SKP) spheres and neurospheres: distinct "stemness" identified by microarray analysis. Cell Reprogram. 12 (3), 329–345.